Effect of thin iridium oxide on the formation of interface dipole in organic light-emitting diodes

Soo Young Kim and Jong-Lam Lee

Citation: Applied Physics Letters **87**, 232105 (2005); doi: 10.1063/1.2135874
View online: http://dx.doi.org/10.1063/1.2135874
View Table of Contents: http://scitation.aip.org/content/aip/journal/apl/87/23?ver=pdfcov
Published by the AIP Publishing

Effect of thin iridium oxide on the formation of interface dipole in organic light-emitting diodes

Soo Young Kim and Jong-Lam Lee[a)]
Department of Materials Science and Engineering, Pohang University of Science and Technology (POSTECH), Pohang, Kyungbuk 790-784, Korea

(Received 19 April 2005; accepted 28 September 2005; published online 29 November 2005)

The 4,4′-bis[N-(1-naphtyl)-N-phenyl-amino]biphenyl was *in situ* deposited on both iridium-oxide-coated indium-tin-oxide (IrO_x–ITO) and O_2-plasma-treated ITO (O_2–ITO), and their interface dipole energies were quantitatively determined using synchrotron radiation photoemission spectroscopy. The dipole energies of both O_2–ITO and IrO_x–ITO were same with each other, −0.3 eV, meaning the formation of same amount of interface dipole. The secondary electron emission spectra revealed that the work function of IrO_x–ITO is higher by 0.5 eV than that of O_2–ITO, resulting in the decrease of the turn-on voltage via reduction of hole injection barrier. © *2005 American Institute of Physics*. [DOI: 10.1063/1.2135874]

Surface-treated indium tin oxide (ITO) has been used as the most common organic light-emitting diode (OLED) anode due to its high transparency, high conductivity, and high work function.[1] To improve the device performance, nanoscale layers of various materials have been deposited between ITO and hole transport layer, such as copper phthalocyanine, dielectrics, polythiophene, and metal oxides with high work functions.[2–5]

The knowledge of barrier heights at interfaces between the electrodes and the organic layers is important for an understanding and improvement of organic semiconductor devices. It is reported that interface dipole (Δ) is formed between metal and organic, organic and organic, due to various origins—such as charge transfer across the interface, redistribution of electron cloud, interfacial chemical reaction, and other types of rearrangement of electronic charge.[6] This Δ shifts the vacuum level at the interface upward or downward. When a metal with a high work function is used as an anode, an interface dipole with its positive pole pointing toward the organic layer and its negative pole toward the metal decreases the metal work function, resulting in the increase of the hole injection barrier.[7,8] However, the effect of a thin hole injection layer of conducting oxide with a high work function on the formation of interface dipole has not been reported yet.

In this letter, we investigated the formation of an interface dipole between iridium oxide (IrO_x)-coated ITO anode and 4,4′-bis[N-(1-naphtyl)-N-phenyl-amino]biphenyl (α-NPD). Synchrotron radiation photoemission spectroscopy (SRPES) was employed to observe the change of the energy level with *in situ* deposition of the α-NPD layer on an IrO_x-coated ITO anode. From this, the effect of the IrO_x layer on the formation of interface dipole in an OLED is discussed.

The glass coating with ITO (150 nm thick, ~20 Ω/cm) was used as the starting substrate. The ITO surface was treated with O_2 plasma for 1 min with a power of 150 *W* (O_2–ITO). Then, 2-nm-thick Ir layer was deposited using rf-magnetron sputter. The Ir film was exposed to O_2 plasma for 1 min to form IrO_x (IrO_x–ITO). The sample was loaded into a thermal evaporator and α-NPD with a thickness of 70 nm, tris(8-hydroxyquinoline) aluminum (60 nm), and aluminum (Al) (150 nm) layers were deposited in sequence. For a reference, a device without IrO_x layer was also prepared. The current density-voltage characteristics of the devices were measured.

For the measurement of SRPES spectra, O_2–ITO and IrO_x–ITO samples were loaded into a vacuum chamber, equipped with the electron analyzer, at 2B1 Beamline in Pohang Accelerator Laboratory. Then, α-NPD was *in situ* deposited on the samples using a thermal evaporator. The evaporation of α-NPD was performed in a separately connected preparation chamber, and core-level spectra, valence-band spectra, and secondary electron emission spectra were obtained in a main chamber using an incident photon energy of 600 eV. The onset of photoemission was measured with a negative bias (−20 V) on the sample to avoid the work function of the detector. The incident photon energy was calibrated with the core-level spectrum of Au 4*f*.

Figure 1 shows current density-voltage characteristics of the two types of devices. Turn-on voltage (V_T) was determined by extrapolating two solid lines from background and straight onset in current density-voltage curve. The V_T of OLEDs using IrO_x–ITO decreased from 7 V to 4 V. Furthermore, the current density of OLED using IrO_x–ITO is

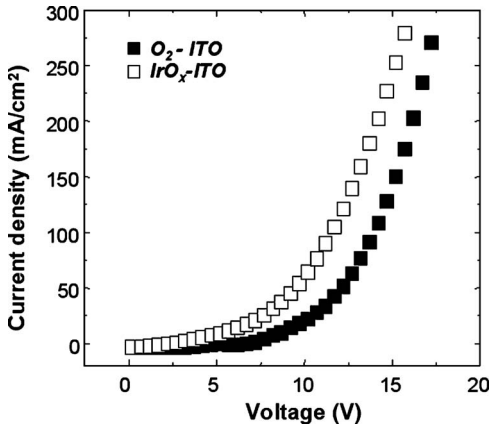

FIG. 1. Current density-voltage characteristics of OLEDs with different anodes.

a)Electronic mail: jllee@postech.ac.kr

TABLE I. Summary of the electroluminescence performance of devices.

Current density (mA/cm^2)	Luminance (cd/m^2)		Current efficiency (cd/A)		Power efficiency (lm/W)	
	O_2–ITO	IrO_x–ITO	O_2–ITO	IrO_x–ITO	O_2–ITO	IrO_x–ITO
20	388	437	1.52	1.71	0.40	0.60
40	681	846	1.53	1.91	0.34	0.57
60	928	1201	1.46	1.88	0.31	0.52
80	1110	1532	1.34	1.85	0.27	0.49
100	1207	1736	1.18	1.70	0.23	0.43

higher than that using O_2–ITO at the same applied voltage. The electroluminescence properties of devices are summarized in Table I. It is shown that luminance, current efficiency, and power efficiency of OLEDs using IrO_x–ITO is superior to that using O_2–ITO at the same current density. Therefore, it is thought that holes were effectively injected from IrO_x–ITO to α-NPD, reducing the V_T and increasing the electroluminescence property of OLEDs. It seems that the device current and power efficiency are quite low. It is thought that the work function of the Al cathode (~4.2 eV) is higher than that of LiF/Al (Li ~ 2.93) or Mg:Ag one (Mg ~ 3.66), decreasing the device efficiency.[9]

Figure 2 shows the change of C 1*s* SRPES spectra according to the deposition steps of α-NPD on [Fig. 2(a)] O_2–ITO and [Fig. 2(b)] IrO_x–ITO. In order to separate the chemical bonding states included in the spectra, the spectral line shape was simulated using a suitable combination of Gaussian and Lorentzian functions. The C 1*s* peak separated into two components. The bulk component of C–O and surface component of C–C were considered. The binding energy of the C–O bond was higher than that of the C–C one, which agrees well with a previously reported value.[10] At the as-deposited state, the C 1*s* peak is wholly composed of the C–O bond. According to deposition of α-NPD on both samples, the peak corresponding to the C–C bond shifted about 0.3 eV toward high binding energy and the peak intensity increased due to the composition of α-NPD. This result showed that the amount of downward band bending is same in both samples.

In order to clarify the change of work function with deposition of α-NPD on O_2–ITO, the SRPES spectra of the secondary electron were measured, as shown in Fig. 3(a). The onset of the secondary electron peak shifted toward lower kinetic energy by 0.6 eV after deposition of α-NPD, meaning the decrease of work function. Figure 3(b) shows the change of valence-band spectra with deposition of α-NPD. The onset of the valence-band maximum (VBM) was determined by extrapolating two solid lines from the background and straight onset in the spectra.[11] Before deposition of α-NPD, the VBM was located at 2.5 eV, showing that the energy difference between the VBM of O_2–ITO and Fermi level (E_F) is 2.5 eV. After deposition of α-NPD, the VBM was located at 2.1 eV, meaning that the energy difference between highest occupied molecular orbital (HOMO) and E_F of α-NPD on O_2–ITO is 2.1 eV. This result showed that hole injection barrier from O_2–ITO to α-NPD is 2.1 eV.

Figure 4(a) shows the change of work function with deposition of α-NPD on IrO_x–ITO. The onset of the secondary electron peak shifted toward lower kinetic energy about 0.6 eV after deposition of α-NPD, meaning the decrease of work function. The change of the VBM with the deposition of α-NPD was shown in Fig. 4(b). Before deposition of α-NPD on IrO_x–ITO, the VBM located at 0.3 eV due to the

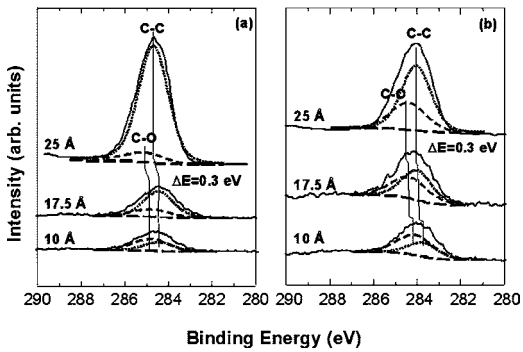

FIG. 2. C 1*s* core-level spectra for (a) O_2–ITO and (b) IrO_x–ITO.

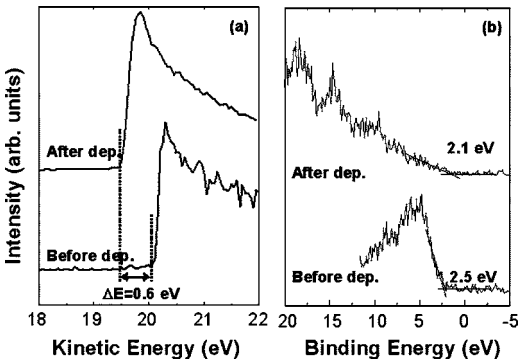

FIG. 3. (a) Secondary electron emission spectra and (b) valence-band spectra for O_2-ITO.

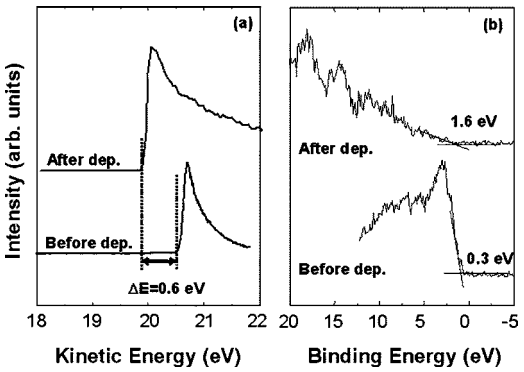

FIG. 4. (a) Secondary electron emission spectra and (b) valence-band spectra for IrO_x–ITO.

TABLE II. Relative atomic concentration of In/C, C–O bonds, and C–C bonds.

		O_2–ITO		IrO_x–ITO	
	In/C	C–O bond	C–C bond	C–O bond	C–C bond
As-deposited	3.35	1	0	1	0
10 Å	3.00	0.61	0.39	0.64	0.37
17.5 Å	2.18	0.27	0.73	0.47	0.53
25 Å	0	0.08	0.92	0.01	0.99

band gap of IrO_x. After deposition of α-NPD, the VBM was located at 1.6 eV, meaning that the HOMO level of α-NPD was located at 1.6 eV apart from E_F. This result indicated that hole injection barrier from IrO_x–ITO to α-NPD is 1.6 eV.

The relative concentrations of In/C, C–O bond, and C–C bond in each step were calculated from the integration of In 3*d* and C 1*s* spectra and their sensitivity factors, summarized in Table II. As the deposition of α-NPD progressed, In/C and C–O bonds decreased and C–C bonds increased due to the composition of α-NPD. The In/C ratio is 0 at 25 Å α-NPD layer thickness, meaning that the surface is wholly covered by α-NPD.

Based on these experimental observations, the effect of the IrO_x layer on the formation of interface dipole could be explained as below. As the thickness of α-NPD on O_2–ITO increases, the core-level peaks shift to the higher binding energy about 0.3 eV [Fig. 2(a)], indicating the downward band bending in α-NPD along from the interface to the surface. The onset of secondary emission in O_2–ITO shifted to lower kinetic energy about 0.6 eV with deposition of α-NPD [Fig. 3(a)], indicating the decrease of the work function on the surface of α-NPD. Considering the band bending of 0.3 eV toward the α-NPD, Δ is determined to be −0.3 eV, as shown in Fig. 5(a). Figure 5(b) shows the schematic band diagram in the deposition of α-NPD on IrO_x–ITO anode. The work function of IrO_x–ITO is higher by 0.5 eV than that of O_2–ITO, as shown in Figs. 3(a) and 4(a). The amount of band bending and the change of work function with deposition of α-NPD are 0.3 eV [Fig. 2(b)] and 0.6 eV [Fig. 4(a)], respectively. Thus, the value of Δ produced at the interface of IrO_x–ITO with α-NPD corresponds to −0.3 eV, as shown in Fig. 5(b).

It was previously reported that the higher work function of metal substrate, the higher Δ exists due to the more sensitive electron density tail.[7] However, the value of Δ is the same in our case even though the work function of IrO_x–ITO is higher than that of O_2–ITO, as shown in Figs. 5(a) and 5(b). In the metalorganic system, the metal work function could be changed with the surface dipole which originates from the tail of free electrons.[12] The contribution of surface dipole could be modified by the presence of an adsorbate. The 2-nm-thick IrO_x has much fewer free electrons than the metals,[13] resulting in the reduced contribution of surface electron tail. As a result, Δ in IrO_x–ITO coincides with the Δ in O_2–ITO. Consequently, the IrO_x layer plays a role in increasing the work function of electrode, leading to the decrease of the hole injection barrier from 2.1 to 1.6 eV. Therefore, the V_T of OLEDs using IrO_x–ITO decreased from 7 V to 4 V.

In conclusion, we investigated the formation of the interface dipole between the IrO_x–ITO anode and α-NPD. The V_T of the OLED decreased from 7 V to 4 V as the IrO_x layer exists between ITO and α-NPD. SRPES spectra showed that the dipole energies of both O_2–ITO and IrO_x–ITO were same with each other, −0.3 eV. The work function of α-NPD on IrO_x–ITO is higher by 0.5 eV than that on O_2–ITO. Thus, the IrO_x layer lowered the potential barrier for hole injection from ITO to α-NPD, reducing the V_T of OLEDs.

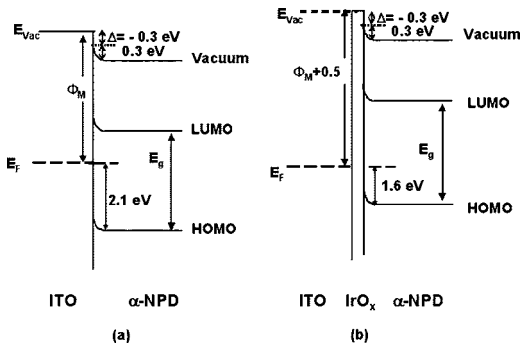

FIG. 5. Schematic band diagram: (a) O_2–ITO and (b) IrO_x–ITO.

This research was supported in part by the Program for the Training of Graduate Students in Regional Innovation which was conducted by the Ministry of Commerce, Industry, and Energy of the Korean Government.

[1] I.-M. Chan, W.-C. Cheng, and F. C. Hong, Appl. Phys. Lett. **80**, 13 (2002).
[2] E. W. Forsythe, M. A. Abkowitz, and Y. Gao, J. Phys. Chem. B **104**, 3948 (2000).
[3] Y. Gao, L. Wang, D. Zhang, L. Duan, G. Dong, and Y. Qiu, Appl. Phys. Lett. **82**, 155 (2003).
[4] P. K. H. Ho, J.-S. Kim, J. H. Burroughes, H. Becker, S. F. Y. Li, T. M. Brown, F. Cacialli, and R. H. Friend, Nature (London) **404**, 481 (2000).
[5] I.-M. Chan, T.-Y. Hsu, and F. C. Hong, Appl. Phys. Lett. **81**, 1899 (2002).
[6] H. Ishii, K. Sugiyama, E. Ito, and K. Seki, Adv. Mater. (Weinheim, Ger.) **11**, 605 (1999).
[7] I. G. Hill, A. Rajagopal, A. Kahn, and Y. Hu, Appl. Phys. Lett. **73**, 662 (1998).
[8] H. Peisert, M. Knupfer, and J. Fink, Appl. Phys. Lett. **81**, 2400 (2002).
[9] D. R. Lide, *CRC Handbook of Chemistry and Physics*, 83rd ed. (CRC Press, Boca Raton, FL, 2002), pp. 12–124.
[10] J. F. Moulder, W. F. Strickle, P. E. Sobol, and K. D. Bomben, *Handbook of X-Ray Photoelectron Spectroscopy* (Perkin–Elmer, Minnesota, Eden Prarie, MN, 1992).
[11] J. M. Baik and J.-L. Lee, Met. Mater. Int. **10**, 555 (2004).
[12] X. Crispin, V. Geskin, A. Crispin, J. Cornil, R. Lazzaroni, W. R. Salaneck, and J.-L. Bredas, J. Am. Chem. Soc. **124**, 8131 (2002).
[13] Z. Qiao, R. Latz, and D. Mergel, Thin Solid Films **466**, 250 (2004).